

## Article

# Vocalization Source Level Distributions and Pulse Compression Gains of Diverse Baleen Whale Species in the Gulf of Maine

Delin Wang, Wei Huang, Heriberto Garcia and Purnima Ratilal \*

Laboratory for Ocean Acoustics and Ecosystem Sensing, Northeastern University, Boston, MA 02115, USA; wang.del@husky.neu.edu (D.W.); huang.wei1@husky.neu.edu (W.H.); garcia.he@husky.neu.edu (H.G.)

\* Correspondence: purnima@ece.neu.edu; Tel.: +1-617-373-8458

Academic Editors: Nicholas Makris, Xiaofeng Li and Prasad S. Thenkabail

Received: 23 June 2016; Accepted: 16 October 2016; Published: 25 October 2016

**Abstract:** The vocalization source level distributions and pulse compression gains are estimated for four distinct baleen whale species in the Gulf of Maine: fin, sei, minke and an unidentified baleen whale species. The vocalizations were received on a large-aperture densely-sampled coherent hydrophone array system useful for monitoring marine mammals over instantaneous wide areas via the passive ocean acoustic waveguide remote sensing technique. For each baleen whale species, between 125 and over 1400 measured vocalizations with significantly high Signal-to-Noise Ratios (SNR > 10 dB) after coherent beamforming and localized with high accuracies (<10% localization errors) over ranges spanning roughly 1 km–30 km are included in the analysis. The whale vocalization received pressure levels are corrected for broadband transmission losses modeled using a calibrated parabolic equation-based acoustic propagation model for a random range-dependent ocean waveguide. The whale vocalization source level distributions are characterized by the following means and standard deviations, in units of dB re 1  $\mu$ Pa at 1 m:  $181.9 \pm 5.2$  for fin whale 20-Hz pulses,  $173.5 \pm 3.2$  for sei whale downsweep chirps,  $177.7 \pm 5.4$  for minke whale pulse trains and  $169.6 \pm 3.5$  for the unidentified baleen whale species downsweep calls. The broadband vocalization equivalent pulse-compression gains are found to be  $2.5 \pm 1.1$  for fin whale 20-Hz pulses,  $24 \pm 10$  for the unidentified baleen whale species downsweep calls and  $69 \pm 23$  for sei whale downsweep chirps. These pulse compression gains are found to be roughly proportional to the inter-pulse intervals of the vocalizations, which are  $11 \pm 5$  s for fin whale 20-Hz pulses,  $29 \pm 18$  for the unidentified baleen whale species downsweep calls and  $52 \pm 33$  for sei whale downsweep chirps. The source level distributions and pulse compression gains are essential for determining signal-to-noise ratios and hence detection regions for baleen whale vocalizations received passively on underwater acoustic sensing systems, as well as for assessing communication ranges in baleen whales.

**Keywords:** baleen whale; vocalization source level; pulse compression

## 1. Introduction

The vocalization behaviors of diverse marine mammal species [1] have been simultaneously monitored over vast areas of the Gulf of Maine using the Passive Ocean Acoustic Waveguide Remote Sensing (POAWRS) technique [1–3] from 19 September–6 October 2006. The marine mammal vocalizations were received on a large-aperture densely-sampled coherent hydrophone array system that provides orders of magnitude higher array gain [4] than a single sensor, enabling whale vocalizations to be detected, localized and classified over an approximately 100,000 km<sup>2</sup> region instantaneously by POAWRS without aliasing in time and space (see the POAWRS detection region for whale vocalizations from diverse species in Figure 3a of [1]).

Here, we estimate the vocalization source levels of four distinct baleen whale species from simultaneous recordings of their vocalizations in the Gulf of Maine. The four baleen whale species analyzed here are fin whale (*Balaenoptera physalus*), sei whale (*Balaenoptera borealis*), minke whale (*Balaenoptera acutorostrata*) and an Unidentified Baleen Whale Species (UBWS). Each baleen whale species was identified from its characteristic vocalization type: the fin whales were identified from their short duration 20-Hz center frequency calls [5–8]; the sei whales from their downsweep chirps occurring singly or as doublets with roughly a 4-s separation or sometimes as triplets [9–11]; and the minke whales were identified from their pulse trains [12–14] comprised of a series of click sequences (see Figure 1 here and also the Extended Data Figures 1–4 of [1]). The unidentified baleen whale species vocalized downsweep signals in the 30–60 Hz frequency range over a 2–3-second duration (see Figure 1J here and the Extended Data Figures 1B and 3A of [1]). These vocalizations have distinct bearing versus time trajectories and localizations that do not follow or coincide well with those of the other baleen whale species present in the area, namely fin, sei, humpback and minke (see the Extended Data Figure 4 of [1]). The unidentified baleen whale species downsweep signals most closely resemble the audible downsweep, burp and grunt calls of blue whales recorded in the Gulf of St. Lawrence [15], a neighboring region to the Gulf of Maine, and they were attributed to blue whales in [1].

For each baleen whale species, between 125 and over 1400 measured vocalizations with significantly high Signal-to-Noise Ratios (SNR > 10 dB) are included in the source level estimation. The source level of each baleen whale vocalization is estimated from the received vocalization pressure level by compensating for corresponding broadband transmission loss [1,16–18] from whale location to the receiver array center location [19–21] in the temporally- and spatially-varying Gulf of Maine environment. The whale locations for each species were previously determined using the moving array triangulation [2,22,23], the bearings-migration minimum mean square error and the array invariant techniques [2,22–24] from the measured bearing versus time trajectories of sequences of vocalizations from that species [1]. The marine mammal species-dependent vocalization source level is an important parameter for estimating the marine mammal detection region for a given species in any passive underwater acoustic sensing system [1,2,25]. It is also employed in distance sampling estimates of marine mammal call density and abundance estimation [26–30]. Vocalization source level is also essential for determining marine mammal communication ranges, which are key considerations in assessing the impact of anthropogenic sound on marine mammal behavior [31,32].

Previous estimates of vocalization source level for the baleen whale species considered here include fin whales off the Western Antarctic Peninsula and near Juan de Fuca Ridge of the northeast Pacific Ocean [33,34]; sei whales on the continental shelf off New Jersey [35]; minke whales near the Great Barrier Reef, Hawaii, and the Stellwagen Bank area of the Gulf of Maine [28,36,37]; and blue whales distributed in multiple ocean areas, including both the Pacific and Atlantic Ocean [15,33,38–40]. Previous vocalization source level estimates typically focused on a single species based on vocalization sample sizes ranging from a few tens to a few hundred. Transmission losses  $TL$  were often modeled previously using the azimuthally-symmetric formula  $TL = X \log_{10} R$  with the transmission loss coefficient  $X$  varying between the limits of spherical spreading ( $X = 20$ ) and cylindrical spreading ( $X = 10$ ) for source-receiver range separation  $R$  depending on the environment [15,33,36,37]. In [35], a normal-mode based ocean acoustic propagation model was employed to correct for transmission losses in estimating sei whale vocalization source level in the shallow New Jersey shelf environment.

Here, we provide vocalization source level estimates for each of the baleen whale species considered using vocalization sample sizes that range from several hundred to a couple of thousand. The transmission losses calculated here are broadband and employ a calibrated [16,41] parabolic equation-based Range-dependent Acoustic propagation Model (RAM) [42] to compute the acoustic field moments in a fluctuating ocean waveguide with complex bathymetry. The model accounts for significant azimuth- and range-dependent variation in transmission losses for the Gulf of Maine environment where water depths can vary drastically from greater than 200 m in the basins to less than 30 m on the banks. While the azimuthally-symmetric ocean acoustic transmission loss formulation used

in previous studies is valid for short ranges and for environments with negligible range dependence, here we find it necessary to employ a range- and depth-dependent acoustic propagation model [42] to handle the effects of significant bathymetric variations and depth-dependent water-column sound speed structure on the propagated marine mammal vocalization intensities received at long ranges.

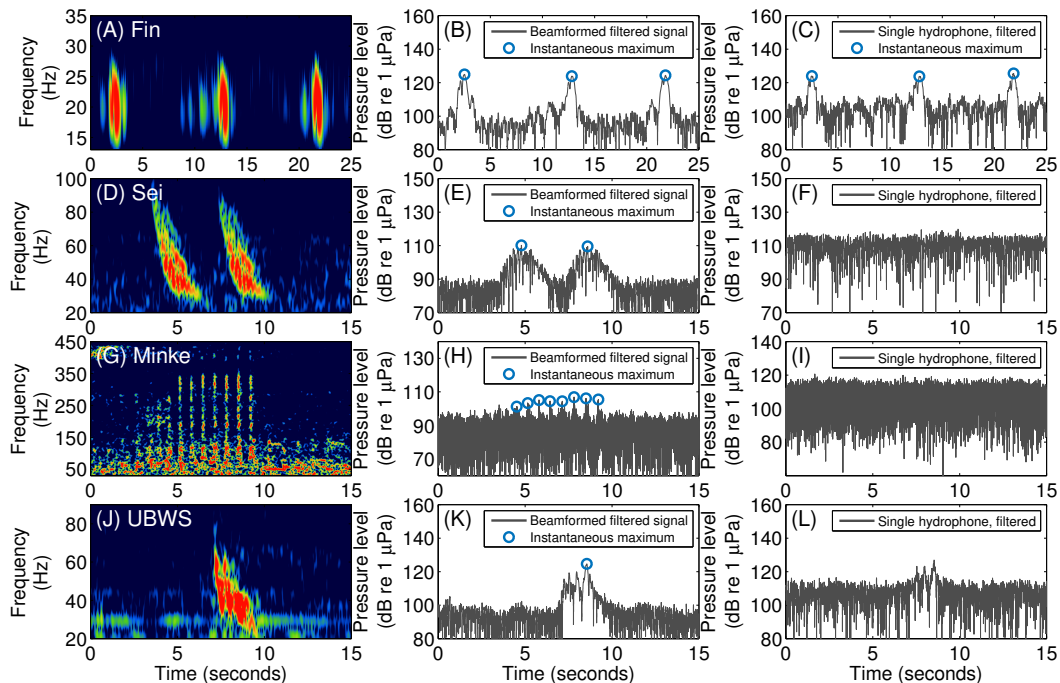


**Figure 1.** Example vocalizations from (A–C) fin whale, (D–F) sei whale, (G–I) minke whale and (J–L) the unidentified baleen whale species. Sub-plots (A,D,G,J) show the beamformed spectrogram of the vocalizations from each species. Corresponding beamformed pressure-time series used for plotting the spectrograms are shown in (B,E,H,K), respectively. (C,F,I,L) show the pressure-time series from a single omnidirectional hydrophone. All signals were bandpass filtered between upper  $f_U$  and lower  $f_L$  frequencies defined as  $-10$  dB end points in power spectrum. The received vocalization pressure levels were estimated from the root-mean-square value of the maximum instantaneous beamformed bandpass filtered pressure-time series. A high gain of up to 18 dB can be achieved after beamforming the data measured on a 64-element sub-aperture of the 160-element hydrophone array, enabling vocalizations from sei whales, minke whales and unidentified baleen whales species to be detected above the ambient noise. In contrast, the sei whale, minke whale and unidentified baleen whale species vocalizations could not be consistently detected on a single hydrophone. For fin whales, since the acoustic wavelengths of the vocalizations are large, the array aperture is not long enough to provide gains larger than 5 dB. The high intensity fin whale 20-Hz pulses are detectable even without coherent beamforming.

The pulse compression gains of the broadband vocalizations are estimated for three baleen whale species: fin whale, the unidentified baleen whale species and sei whale. The pulse compression gain is quantified as the ratio of the signal duration to the width of the main-lobe after vocalization frequency modulation to the baseband and matched filtering operations. Sonar, radar and ultrasonic systems [43,44] often employ pulse compression to enhance signal-to-noise ratios in signal detection and range-resolution in imaging applications. Marine mammal vocalization pulse compression gains are required for determining detection regions in underwater passive single sensor [45–48] or array sensor systems [1,2,22] that employ match-filter operations to enhance vocalization detection, as well as vocalization arrival time and bearing estimation for localization applications [1,3,22].

## 2. Material and Methods

### 2.1. Gulf of Maine 2006 Experiment Acoustic Data Collection

The Gulf of Maine is an important North Atlantic marine mammal foraging ground and contains a number of significant spawning areas for various fish species [49–51], including the Atlantic herring (*Clupea harengus*) [52–54]. The Atlantic herring comprises a keystone prey species, common in the diets of many marine mammals, piscivorous fish and seabirds of the region [52,55]. The spawning activity of Atlantic herring on the northern flank of Georges Bank during the fall season each year has been observed [52,53,56–58] and recorded by the U.S. National Marine Fisheries Services (NMFS) for over 30 years, coinciding with their annual survey of the Georges Bank herring stock with this period each year.

The Gulf of Maine 2006 Experiment [1,2,16,17,22,23,41,59–61] was conducted from 19 September–6 October 2006, in conjunction with the US NMFS annual Atlantic herring acoustic survey of the Gulf of Maine and Georges Bank. The Atlantic herring areal population densities were monitored over instantaneous wide areas using active OAWRS imaging [1,2,16,17,60] and calibrated with coincident conventional ultrasonic fisheries echo sounding measurements [16,17,60] with fish species identification and physiological parameters extracted from trawl samples collected over the course of the experiment [56,62]. The overall Georges Bank Atlantic herring stock estimate for autumn 2006 based on the OAWRS survey has been found to match well (with 80%–90% agreement) with independent NMFS stock estimates for 2006 and 2007 [61].

During the experiment, acoustic recordings were acquired using a 160 hydrophone-element horizontal receiver line-array towed behind a research vessel along designated tracks north of Georges Bank [2,16,17,41]. To minimize the effect of tow ship noise on the recorded acoustic data, the coherent hydrophone array was towed approximately 375–405 m behind the research vessel so as to confine this noise to the forward end-fire direction of the array. The tow ship noise in directions away from the forward end-fire was negligible after coherent beamforming. The omnidirectional ambient noise spectral levels in the frequency band of the vocalizations for each baleen whale species considered here are provided in the Supplementary Information Section I of [1]. The acoustic recordings of the coherent hydrophone array system contained marine mammal vocalizations from over eight distinct whale species [1,2] that include fin, humpback, sei, minke, orca, pilot, sperm, as well as other unidentified baleen and toothed whale species. Here, we focus our analysis on vocalizations of the fin whale, sei whale, minke whale and an unidentified baleen whale species recorded on the coherent hydrophone array.

Data from all 160 hydrophone elements nested into four sub-apertures are used, where each sub-aperture contains 64 hydrophones for spatially- and temporally-unaliased sensing up to 4 kHz (the sampling rate of POAWRS was 8 kHz). Detailed specifications of the coherent hydrophone array and data acquisition system used here are provided in [1,2,16,22,23,41,63], including array layout and aperture nesting. The low-frequency (LF) aperture, with inter-element spacing of 1.5 m, was used to analyze baleen whale vocalizations with fundamental frequency content below 500 Hz. The instantaneous receiver array center positions are determined from the shipboard Global Positioning System (GPS). The water-column temperature and salinity were measured using Expendable Bathythermographs (XBTs) and Conductivity-Temperature-Depth (CTD) sensors. Other details about the measurement geometry and oceanographic properties of the environment are provided in Section II of [16] and also in [1,2,17,22,23,41,59,64].

### 2.2. Baleen Whale Vocalization Detection and Classification

Acoustic pressure-time series measured by sensors across the receiver array were converted to two-dimensional (2D) beam-time series by conventional time-domain beamforming [4] and further converted to spectrograms by short-time Fourier transform (0.26-s length, 75% overlap, Hanning window). The baleen whale vocalizations were automatically extracted from the

beamformed spectrograms using a threshold detector ( $>5.6$  dB SNR) and checked by visual inspection [1]. The azimuthal bearing of each extracted vocalization was subsequently determined by selecting the bearing in which the beamformed, bass-pass filtered pressure-time series contained maximum energy during the time duration of the vocalization and in the same frequency band. With our densely-sampled, large-aperture coherent POAWRS receiver array, a high gain of up to  $10 \log_{10} n = 18$  dB where  $n = 64$  hydrophones for each sub-aperture can be achieved, enabling the detection of baleen whale vocalizations up to two orders of magnitude more distant in range in the shallow water environment than a single omnidirectional hydrophone, which has no array gain (Figure 1). The actual array gain, which may be smaller than the full 18-dB array gain, is dependent on noise coherence and vocalization wavelength relative to array aperture length.

From the beamformed spectrograms, the time-frequency characteristics of each baleen whale vocalization were extracted via pitch tracking [1,10,65,66] and applied for species classification. A pitch track describes the time-variation of the fundamental frequency in the vocalization signal. It consists of a time series  $t = (t_1, t_2, \dots, t_i)$ , a frequency series  $f = (f_1, f_2, \dots, f_i)$  and an amplitude series  $A = (A_1, A_2, \dots, A_i)$ , determined using a time-frequency peak detector from the beamformed spectrogram, which is created from short-time Fourier transforms of the audio data (sampling frequency = 8000 Hz, frame = 526 samples, overlap = 1/2, Hann window). A combination of extracted features from pitch-tracking, orthogonalized via Principle Component Analysis (PCA) [67], were used to optimize the vocalization species classification employing k-means [68] and Bayesian-based Gaussian mixture model clustering approaches [1]. The number of clusters can be determined via the Bayesian Information Criterion (BIC). The eight features extracted from baleen whale vocalization pitch-tracking are provided in the Extended Data Table 2 of [1] for the species examined here. The bearing-time trajectories of each closely-associated series of vocalizations were also taken into account to ensure consistent classification.

### 2.3. Localization of Baleen Whale Vocalizations

The horizontal location of each detected baleen whale vocalization consists of a range and a bearing estimate. The estimated azimuthal bearings of sequences of baleen whale vocalizations form multiple bearing-time trajectories (Figure 2). These bearing-time trajectories are utilized to determine the ranges of the baleen whale vocalizations from the horizontal receiver array center employing the Moving Array Triangulation (MAT) [2,22,23] and the bearings-migration Minimum Mean Square Error (MMSE) methods [22]. Position estimation error or the root mean squared (rms) distance between the actual and estimated location is a combination of range and bearing errors quantified for this array in [2,22,23]. Range estimation error, expressed as the percentage of the range from the source location to the horizontal receiver array center, for the MAT and MMSE is roughly 2% at array broadside and gradually increases to 10% at  $65^\circ$  from broadside and 25% near or at end-fire. Bearing estimation error of the time-domain beamformer ranges from  $0.1^\circ$ – $1.4^\circ$  at array broadside and gradually increases to between  $0.7^\circ$  and  $5.3^\circ$  at end-fire depending on the frequency of the vocalizations [1,16,69] for the given array aperture. These errors are determined at the same experimental site and time period as the marine mammal position estimates presented here, from thousands of controlled source signals transmitted by a source array, and are based on absolute GPS ground truth measurements of the source array's position [22,23], which are accurate to within 3 m–10 m. More than 80% of vocalizations are found to originate from between  $0^\circ$  and  $65^\circ$  of the array broadside direction, where both the MAT and MMSE offered reliable and consistent localization estimates. Vocalizations for which the MAT mean and the MMSE localization estimates differed by more than 10% of the estimated range were removed from all further analysis.



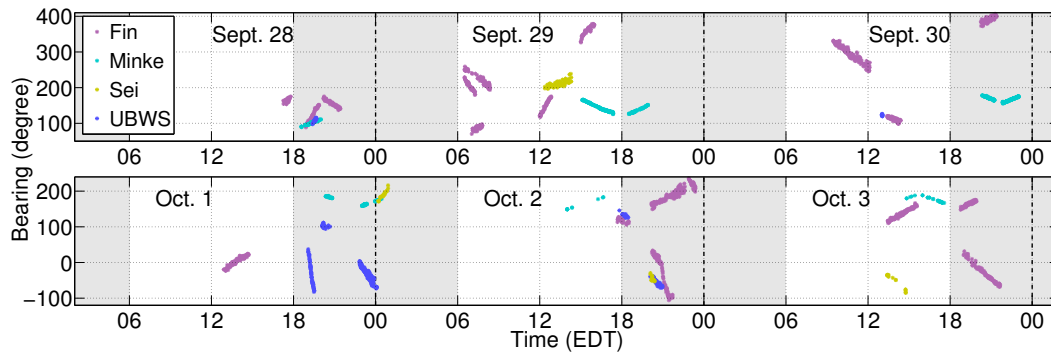


**Figure 2.** The bearing-time trajectories of four distinct baleen whale species: fin whale, minke whale, sei whale and unidentified baleen whale species. One thousand four hundred and ten fin whale vocalizations, 431 minke whale pulse trains, 125 sei whale vocalizations and 417 unidentified baleen whale species vocalizations were selected to estimate the species-dependent baleen whale vocalization source levels. These vocalizations are a subset of the larger set of baleen and toothed whale vocalizations measured by the POAWRS receiver array for each species (see the Extended Data Figures 1–4 of [1]). The bearings are measured with respect to true north.

#### 2.4. Broadband Transmission Loss Modeling

The corresponding one-way broadband acoustic transmission loss from the estimated location of each whale vocalization to the center of the POAWRS receiver array was calculated following the approach described in Section I of the Supplementary Information of [1]. A calibrated [16,41] parabolic equation-based Range-dependent Acoustic propagation Model (RAM) [42] was employed to calculate the broadband transmission loss via [16,18,41,70]:

$$TL(|\mathbf{r} - \mathbf{r}_0|) = 10 \log_{10} \left( \int_{f_L}^{f_U} Q(f) \langle |G(\mathbf{r}|\mathbf{r}_0, f)|^2 \rangle df \right) \quad (1)$$

where  $G(\mathbf{r}|\mathbf{r}_0, f)$  is the waveguide Green function at frequency  $f$  for a whale located at  $\mathbf{r}_0$  and the receiver at  $\mathbf{r}$ ,  $Q(f)$  is the normalized vocalization spectra and  $f_U$  and  $f_L$  are the upper and lower frequencies used for the bandpass filter. The model takes into account the environmental parameters, such as the range-dependent water depth and sound speed profiles, to stochastically compute the propagated acoustic intensities (Figure 3) via Monte Carlo simulations following the approach of [16,18,70]. The mean magnitude-squared waveguide Green function is obtained by averaging over multiple whale depths from the sea surface to the sea floor and over multiple Monte Carlo simulations to account for the unknown whale depth and waveguide fluctuations. The broadband transmission loss standard deviations are calculated in the log-transformed domain using the broadband transmission loss at each potential whale depth from the sea surface to the seafloor.

#### 2.5. Source Level Estimation

The baleen whale vocalization source level  $SL$  is estimated (Figures 4–7) using the passive sonar equation [2,19,71],

$$SL(\mathbf{r}_0) = RL(\mathbf{r}) + TL(|\mathbf{r} - \mathbf{r}_0|) \quad (2)$$

where  $RL(\mathbf{r}_0)$  is the received whale vocalization pressure level. The received whale vocalization pressure level was estimated as the root mean squared (rms) value of the maximum instantaneous time-domain signal bandpass-filtered between upper  $f_U$  and lower  $f_L$  frequencies and beamformed to the azimuthal bearing of the vocalization, over a time window [72] encompassing 90% of the total signal energy (Figure 1). The upper  $f_U$  and lower  $f_L$  frequencies are determined as the  $-10$  dB end points relative to the signal peak in the power spectrum. The frequency bands bounded by lower  $f_L$  and

upper  $f_U$  frequencies containing 90% of the vocalization signal energies on average are 13 Hz–34 Hz for fin whale 20-Hz pulses, 28 Hz–92 Hz for sei whale double downsweep calls, 66 Hz–463 Hz for minke whale clicks and 25 Hz–70 Hz for the unidentified baleen whale species downsweep calls.

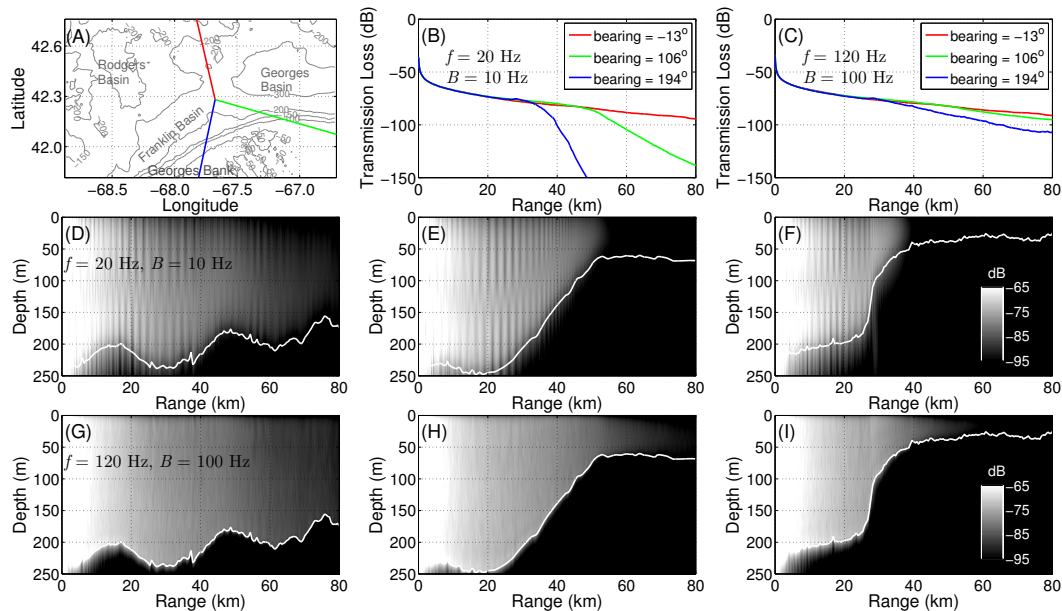


**Figure 3.** Example of broadband transmission losses calculated by a calibrated [16,41] parabolic equation-based range-dependent acoustic propagation model [42] along three propagation paths with the following directions:  $-13^\circ$  (roughly northwards crossing Georges Basin),  $106^\circ$  (roughly eastwards across Georges Bank) and  $194^\circ$  (roughly southwards across Georges Bank), as shown in (A). The transmission losses for two distinct broadband signals centered at 20 Hz and 120 Hz are plotted in (B,C), respectively, as a function of propagation range. The modeled broadband waveguide Green functions averaged over 15 Monte Carlo simulations for each signal along the three propagation directions are shown in (D–F,G–I), respectively, for the two broadband signals. The Green functions are used to calculate the transmission losses shown in (B,C) by averaging over multiple depths from the sea surface to near the sea floor to account for unknown whale depth.

Due to their high intensities, the fin whale 20-Hz pulses were also detectable in the unbeamformed bandpassed-filtered pressure-time series measured by each omnidirectional element of the hydrophone array (Figure 1C). The received pressure levels of fin whale vocalizations without beamforming ( $RL_{unbf}$ ) are estimated as the maximum value out of the 160 received bandpass-filtered pressure levels on each element of the hydrophone array. The unbeamformed received pressure levels are compared to the received pressure levels with beamforming. For the pulse trains from minke whales, source level results are reported as  $SL_{click}$  and  $SL_{max}$ , which are the source levels of the individual clicks or units within pulse trains and the maxima of all of the clicks or units in a pulse train, respectively. The baleen whale species source level estimates here are based on rms quantities.

## 2.6. Pulse Compression Gain Estimation

Pulse compression [43,44] is widely employed in radar, sonar and ultrasonic systems to enhance signal-to-noise ratios in signal detection and range-resolution in imaging applications. A frequency or phased modulated long pulse can be compressed by matched filtering the received signal with a replica of the modulated pulse signal. The Pulse Compression Gain (PCG) [43]  $\gamma$  is a measure of the degree to which the pulse can be compressed and is defined as the ratio of the original uncompressed pulse width  $\tau$  to the pulse width  $\tau_c$  after pulse compression. For a typical Linear Frequency Modulated (LFM) pulse with duration  $\tau$ , it can be compressed to a duration  $\tau_c = 1/B$  after matched filtering,

where  $B$  is the modulated pulse spectral bandwidth [43]. The LFM pulse then has a pulse compression gain given by  $\gamma = \frac{\tau}{\tau_c} = \tau B$ , which is the time-bandwidth product [73,74].

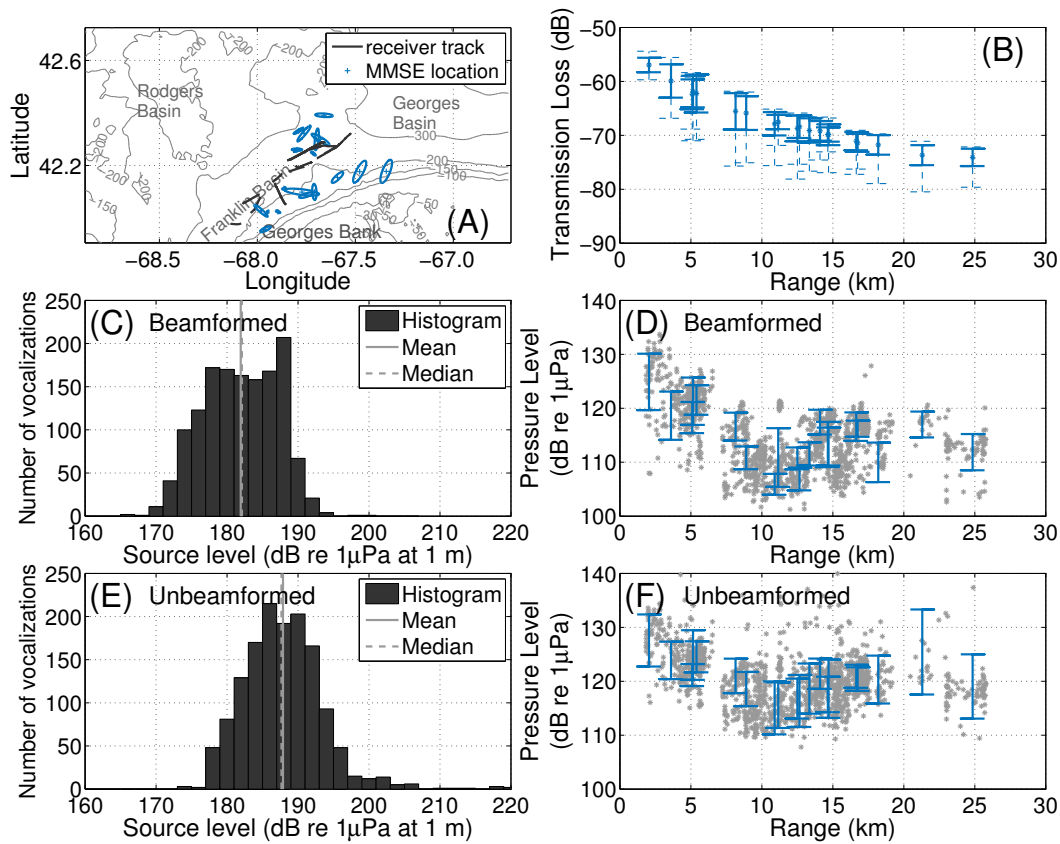


**Figure 4.** (A) The MMSE estimated center locations of sequences of fin whale vocalizations from 20 distinct bearing-time trajectories containing a total of 1410 vocalizations. The localization range and bearing errors are shown by the ellipse; (B) Corresponding one-way broadband transmission losses from the MMSE estimated fin whale vocalization sequence center locations to the POAWRS receiver array center. The transmission loss standard deviations (solid bar), minimum and maximum values (dotted bar) are calculated assuming the whales are located at each potential depth from the sea surface to near the seafloor; (C) Distribution of fin whale vocalization source level derived from bandpass-filtered beamformed signals has a mean of  $181.9 \pm 5.2$  dB re  $1 \mu\text{Pa}$  at 1 m; (D) The received fin whale vocalization pressure levels estimated from beamformed data are plotted as a function of distance from estimated instantaneous MAT locations of each vocalization to the receiver array center. These data are used to derive the source level distribution shown in (C); (E) Distribution of fin whale vocalization source level derived from bandpass-filtered unbeamformed signals has a mean of  $187.9 \pm 5.6$  dB re  $1 \mu\text{Pa}$  at 1 m; (F) The maximum value of the fin whale vocalization pressure levels received on 160 hydrophone elements of the POAWRS receiver array used to derive the source level distribution shown in (E). The blue bars in (D,F) represent one standard deviation in the pressure levels for each bearing-time trajectory.



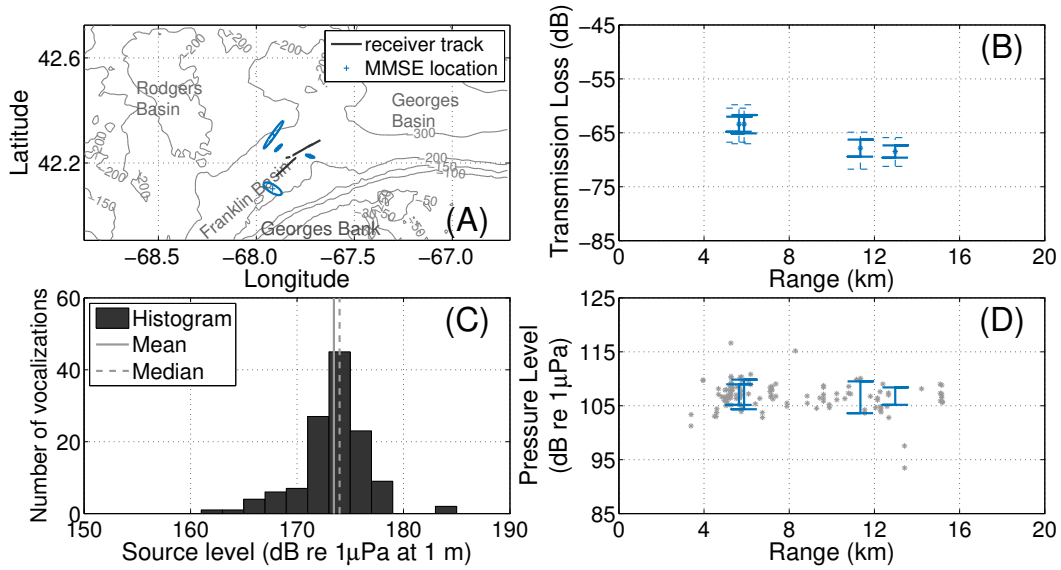


**Figure 5.** (A) The MMSE estimated center locations of sequences of sei whale vocalizations from 4 distinct bearing-time trajectories containing a total of 125 vocalizations; (B) Corresponding one-way broadband transmission losses from the MMSE estimated sei whale vocalization sequence center locations to the POAWRS receiver array center. The transmission loss standard deviations (solid bar), minimum and maximum values (dotted bar) are calculated assuming the whales are located at each potential depth from the sea surface to near the seafloor; (C) Distribution of sei whale vocalization source level derived from bandpass-filtered beamformed signals has a mean of  $173.5 \pm 3.2$  dB re  $1 \mu\text{Pa}$  at 1 m; (D) The received sei whale vocalization pressure levels estimated from beamformed data plotted as a function of the distance from the estimated instantaneous MAT location of each vocalization to the receiver array center. These data are used to derive the source level distribution shown in (C). The blue bars in (D) represent one standard deviation in the pressure levels for each bearing-time trajectory.

Each baleen whale vocalization can be considered as a nonlinear frequency modulated pulse, and the PCG is estimated by matched filtering the received signal with a normalized replica generated following the approach described in Appendix B of [22]. Vocalization bandwidth  $B$  is calculated as the difference between the upper  $f_U$  and lower  $f_L$  frequencies used for the bandpass filter during source level estimation. The uncompressed pulse width  $\tau$  is estimated as the length of the time window encompassing 90% of the total signal energy. After modulating or shifting the broadband vocalizations within  $[f_L, f_U]$  to baseband  $[0, f_U - f_L]$ , the matched filter output (Figure 8) is calculated using Equation (3) of [18]:

$$\begin{aligned}
 MF(\mathbf{r}|\mathbf{r}_0, t_M) &= |h(t|t_M) * \Psi(\mathbf{r}|\mathbf{r}_0, t)|^2 \\
 &= \left| \int_{f_L}^{f_U} \Phi(\mathbf{r}|\mathbf{r}_0, f) H(f|t_M) \exp(j2\pi f t) df \right|^2 \\
 &= \left| \int_{f_L}^{f_U} \Phi(\mathbf{r}|\mathbf{r}_0, f) K Q^*(f) \exp(j2\pi f (t - t_M)) df \right|^2
 \end{aligned} \tag{3}$$

where  $\Psi(\mathbf{r}|\mathbf{r}_0, t)$  is the received vocalization pressure at time  $t$  at receiver location  $\mathbf{r}$  from a whale at  $\mathbf{r}_0$  with vocalization complex spectral amplitude  $\Phi(\mathbf{r}|\mathbf{r}_0, f)$  at frequency  $f$ . The normalized matched filter is given by  $h(t|t_M) = Kq(t_M - t)$ , and its Fourier transform is  $H(f|t_M) = KQ^*(f) \exp(-j2\pi f t_M)$ , where  $t_M$  is the delay time of the matched filter,  $q(t)$  is the received vocalization signal,  $Q(f)$  is the Fourier transform of that signal and  $K = (\int_{f_L}^{f_U} |Q(f)|^2 df)^{-1/2}$  is the normalizing factor.

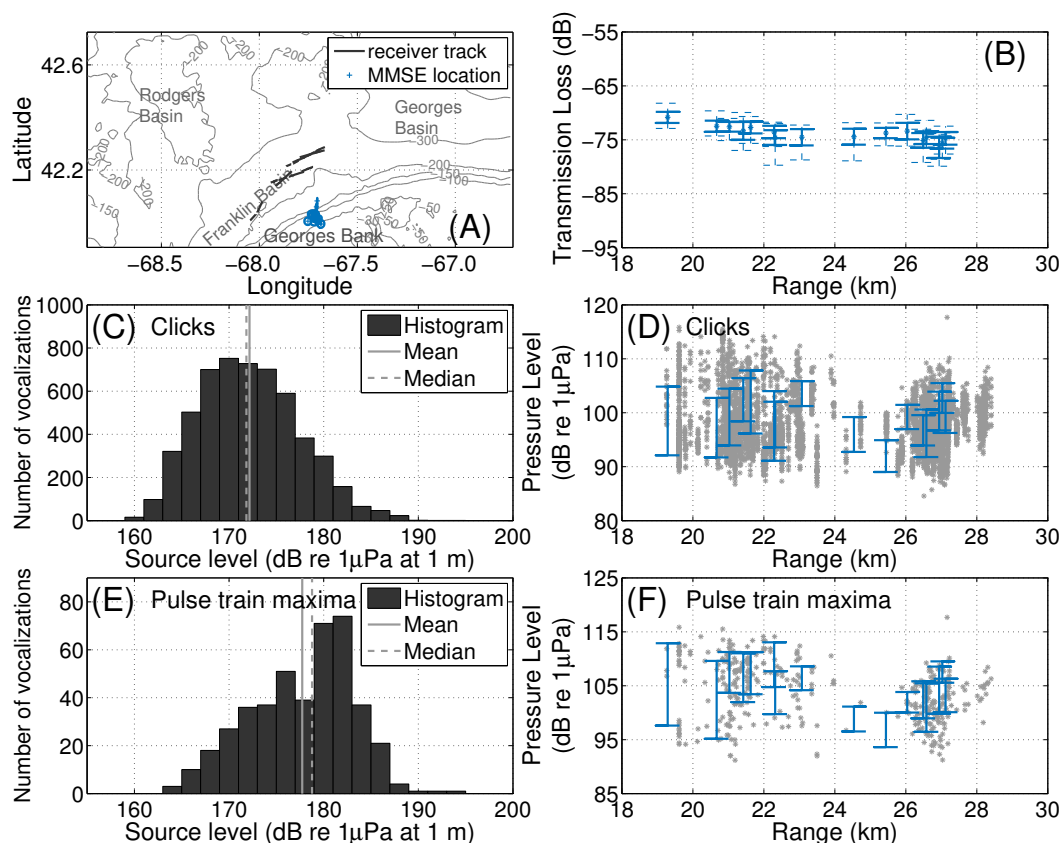


**Figure 6.** (A) The MMSE estimated center locations of sequences of minke whale pulse train vocalizations from 16 distinct bearing-time trajectories consisting of a total of 431 pulse trains and 5390 clicks; (B) Corresponding one-way broadband transmission losses from the MMSE estimated minke whale vocalization sequence center locations to the POAWRS receiver array center. The transmission loss standard deviations (solid bar), minimum and maximum values (dotted bar) are calculated assuming the whales are located at each potential depth from the sea surface to near the seafloor; (C) The distribution of the individual minke whale click vocalization source level estimated from bandpass-filtered beamformed signals has a mean of  $172.2 \pm 5.3$  dB re  $1 \mu\text{Pa}$  at 1 m; (D) The corresponding received click pressure levels are plotted as a function of distances from instantaneous MAT location estimates to the receiver array center. The blue bars represent one standard deviation in the pressure levels estimation; (E) The distribution of the maximum minke whale vocalization source level obtained from the maxima of the click source level in each pulse train has a mean of  $177.7 \pm 5.4$  dB re  $1 \mu\text{Pa}$  at 1 m; (F) The maximum beamformed received pressure levels of each minke whale pulse train used to derive the distribution in (E). The blue bars in (D,F) represent one standard deviation in the pressure levels for each bearing-time trajectory.

The compressed baleen whale vocalization pulse width  $\tau_{c,-6\text{dB}}$  is estimated from the matched filter output as the time duration corresponding to the  $-6$  dB down in  $10 \log_{10}$  of the matched filter output (Equation (3)) on both sides of the peak. The compressed baleen whale vocalization equivalent pulse width  $\tau_{c,eq}$  is also reported. The mean PCGs,  $\gamma_{-6\text{dB}}$  and  $\gamma_{eq}$ , estimated from the vocalizations of each baleen whale species are compared with the time-bandwidth product  $\tau \cdot B$ , which is the pulse compression gain for LFM pulses. In the vocalization pulse compression gain estimation, the time-domain signal was always bandpass filtered and further beamformed to the azimuthal bearing of the vocalization in the same way as in the source level estimation.

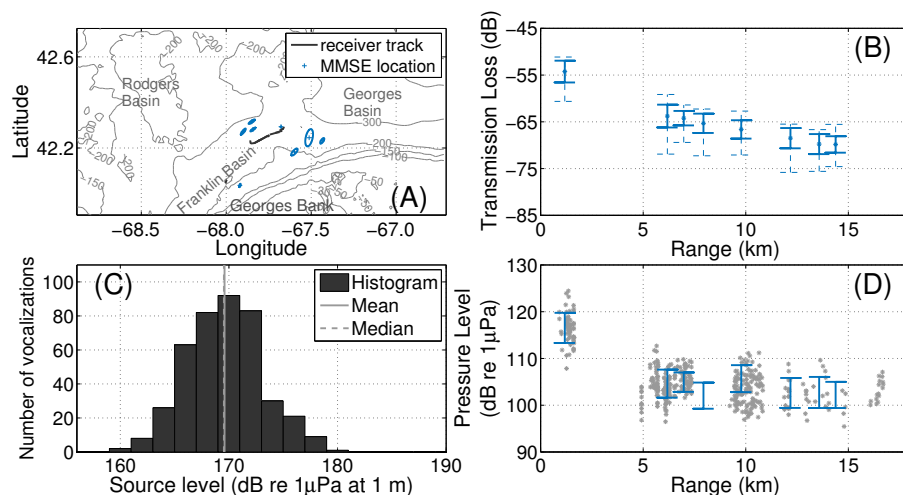


**Figure 7.** (A) The MMSE estimated center locations of sequences of the unidentified baleen whale species downsweep vocalizations from 8 distinct bearing-time trajectories containing a total of 417 vocalizations; (B) Corresponding one-way broadband transmission losses from the MMSE estimated unidentified baleen whale species vocalization sequence center locations to the POAWRS receiver array center. The transmission loss standard deviations (solid bar), minimum and maximum values (dotted bar) are calculated assuming the whales are located at each potential depth from the sea surface to near the seafloor; (C) The distribution of the unidentified baleen whale species vocalization source level derived from bandpass-filtered beamformed signals has a mean of  $169.6 \pm 3.5$  dB re  $1 \mu\text{Pa}$  at 1 m; (D) The received unidentified baleen whale species vocalization pressure levels estimated from beamformed data plotted as a function of the distance from estimated instantaneous MAT locations of each vocalization to the receiver array center. These data are used to derive the source level distribution shown in (C). The blue bars in (D) represent one standard deviation in the pressure levels for each bearing-time trajectory.

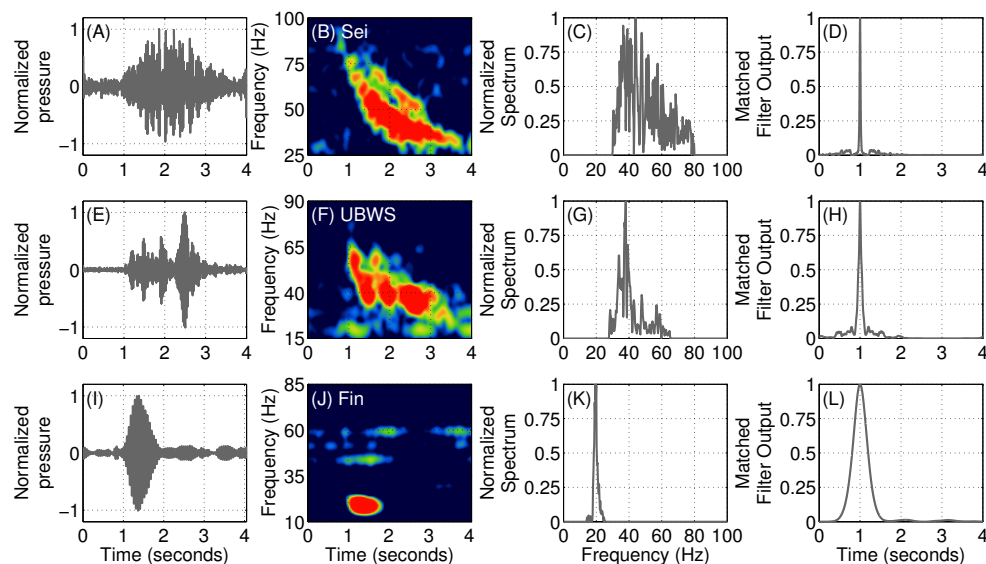


**Figure 8.** Example vocalizations and corresponding matched filter outputs for (A–D) sei whale, (E–H) unidentified baleen whale species and (I–L) fin whale. Sub-plots (A,E,I) show the beamformed pressure-time series for each species. The corresponding spectrograms (0.26-s length, 75% overlap) are shown in (B,F,J), respectively. Sub-plots (C,G,K) show the normalized spectrum for each vocalization over a time-window encompassing 90% of the total energy. After matched filtering each vocalization signal with a corresponding replica generated following the approach described in Appendix B of [22], the compressed pulse signals are plotted in (D,H,L), respectively.

### 3. Results

The baleen whale species-dependent vocalization source levels are estimated using 1410 fin whale vocalizations, 125 sei whale vocalizations, 431 minke whale pulse trains and 417 unidentified baleen whale species vocalizations. These vocalizations were selected based on several criteria that include (1) high Signal-to-Noise Ratios ( $\text{SNR} > 10$  dB); (2) could be reliably localized with high accuracies (the MAT mean and the MMSE localization estimates differed by less than 10% of the estimated range); and (3) the bearing-time trajectories and spectra did not overlap with those of other significant sound sources. The bearing-time trajectories of all selected and classified vocalizations are shown in Figure 2. These vocalizations are a subset of the full set of baleen and toothed whale vocalizations simultaneously measured, detected and classified using the POAWRS approach for each species (see the Extended Data Figures 1–4 of [1] showing the distinct vocalization frequency range and bearing versus time trajectories for a wide variety of marine mammal species detected).

#### 3.1. Fin Whales

The fin whales are identified from their characteristic 20-Hz center frequency high intensity calls [5–8] that have been associated with communication among fin whale individuals [75] and also found to be uttered by males as breeding displays in their mating grounds [5,76] (Figure 1A). Instantaneous azimuthal bearing estimates of the selected 1410 fin whale vocalizations are associated into 20 distinct bearing-time trajectories (Figure 2). The selected fin whale vocalizations are localized to areas on northern Georges Bank and west of Georges Basin, with ranges spanning between 1.9 and 25.8 km (Figure 4A) from the receiver array center.

The corresponding one-way broadband transmission losses are calculated and plotted in Figure 4B as a function of the distance of the MMSE estimated center location of a sequence of fin whale vocalizations (from each bearing-time trajectory) to the center of the POAWRS receiver array. The transmission loss variation during the time duration of a single bearing-time trajectory is ignored. The transmission loss is calculated as  $10 \log_{10}$  of the mean spectrally-weighted magnitude-squared waveguide Green function, which is obtained by averaging over multiple whale depths and over five Monte Carlo simulations per whale depth. The transmission loss standard deviations, minimum and maximum values are calculated assuming the fin whales are located at each potential depth from the sea surface to near the seafloor.

The received fin whale vocalization pressure levels estimated from the beamformed bandpass-filtered time-domain signals are plotted in Figure 4D as a function of the distance of the estimated instantaneous MAT location of each whale vocalization to the receiver array center. The received pressure level standard deviations are calculated for each bearing-time trajectory. This standard deviation is a combination of fluctuations from varying whale depth and range, propagation scintillation in a shallow water waveguide, as well as the source level variation of the vocalizations. The received pressure level standard deviations are expected to be larger than the transmission loss standard deviations. The received vocalization pressure levels are next corrected for the corresponding one-way broadband transmission losses, leading to the fin whale vocalization source level distribution shown in Figure 4C. The average source level estimated from this distribution is  $181.9 \pm 5.2$  dB re 1  $\mu\text{Pa}$  at 1 m over the 13–34-Hz vocalization frequency band of the fin whale.

The received fin whale vocalization pressure levels  $RL_{unbf}$  estimated from the bandpass-filtered time-domain signals without beamforming are shown in Figure 4F. The corresponding fin whale source level  $SL_{unbf}$  distribution derived from these measurements is characterized by a mean of  $187.9 \pm 5.6$  dB re 1  $\mu\text{Pa}$  at 1 m (Figure 4E). The fin whale source level mean derived from the beamformed data is approximately 6 dB smaller than that derived from the unbeamformed data. This is because the time-domain signal after beamforming represents a spatially-averaged signal across the hydrophone elements of the array. In contrast, the source level derived from the unbeamformed data is based on the maximum vocalization pressure level received on the 160 hydrophone elements of the receiver array. Note that the received fin whale vocalization pressure levels shown in Figure 4D,F originate

from locations that span a wide range of azimuths about the receiver array whose locations also vary (Figure 4A). As a result, the received fin whale vocalization pressure levels in Figure 4D,F undergo different transmission loss versus range trends (Figure 3B) leading to the non-monotonic decay with range seen in Figure 4D,F.

### 3.2. Sei Whales

The sei whales were identified from their downsweep calls [9–11], hypothesized to be long-range contact calls potentially enabling coordinated activities, such as feeding [1,10] or breeding [10]. They usually occur singly or as doublets with approximately a 4-s separation (Figure 1D) and sometimes as triplets. Instantaneous bearing estimates of 125 sei whale downsweep calls are associated with four bearing-time trajectories (Figure 2). The sei whale vocalization spatial locations shown in Figure 5A vary between 3.4 and approximately 16 km from the receiver array center. The four vocalization sequences are charted to areas within Franklin Basin. The corresponding one-way broadband transmission losses are plotted in Figure 5B.

The vast majority of received sei whale vocalizations are not intense enough to be detected above the ambient noise floor at each hydrophone without beamforming (see Figure 1D–F). The received sei whale vocalization pressure levels estimated from bandpass-filtered beamformed time-domain signals are shown in Figure 5D. The average source level is estimated to be  $173.5 \pm 3.2$  dB re 1  $\mu$ Pa at 1 m over the 28–92-Hz frequency band of the sei whale vocalizations after correcting for corresponding one-way broadband transmission losses (Figure 5C).

### 3.3. Minke Whales

The minke whales were identified from their pulse trains (Figure 1G) comprised of a series of click sequences [12–14]. Four hundred thirty one pulse trains, consisting of 5390 clicks, are associated with 16 bearing-time trajectories (Figure 2). The vocalization pulse train sequences from all 16 bearing-time trajectories are spatially charted to a focused area on north-central Georges Bank (Figure 6A), with ranges varying between 19.3 and 28.4 km from the receiver array center. The corresponding one-way broadband transmission losses are plotted in Figure 6B.

The pressure levels of individual clicks in the minke whale pulse train, estimated from bandpass-filtered beamformed time-domain signals, are shown in Figure 6D. The received pressure levels of most individual minke whale clicks were not high enough to be detectable from the time-domain signal without coherent beamforming. The minke whale source level  $SL_{click}$  distribution derived from individual minke whale clicks has a mean of  $172.2 \pm 5.3$  dB re 1  $\mu$ Pa at 1 m over the 66–463-Hz frequency band of the vocalizations (Figure 6C).

The maximum source level of minke whale pulse trains  $SL_{max}$ , derived from the maxima of the beamformed clicks in each pulse train, is also calculated (Figure 6F). This source level distribution  $SL_{max}$  has a mean of  $177.7 \pm 5.4$  dB re 1  $\mu$ Pa at 1 m (Figure 6E). Different calling patterns and pulse train types [14] were not separated during the calculations. Thus, the source level distributions shown here are an average over all minke whale vocalization pulse train types detected in the region.

### 3.4. An Unidentified Baleen Whale Species

Instantaneous bearing estimates of 417 downsweep calls of the unidentified baleen whale species are associated with eight bearing-time trajectories (Figure 2) with estimated locations shown in Figure 7A. The unidentified baleen whale species vocalization spatial locations partially overlap with those of the fin whale and have ranges varying between 0.9 and 16.7 km from the POAWRS receiver array. The corresponding one-way broadband transmission losses are plotted in Figure 7B.

The received unidentified baleen whale species downsweep calls are not intense enough to be consistently detected above the ambient noise floor at each hydrophone without beamforming (see Figure 1J–L). Therefore, the received unidentified baleen whale species vocalization pressure levels and standard deviations (Figure 7D) are all estimated from the beamformed bandpass-filtered



time-domain signal. The average source level is estimated to be  $169.6 \pm 3.5$  dB re 1  $\mu$ Pa at 1 m over the 25–70-Hz frequency band of the unidentified baleen whale species downsweep vocalizations after correcting for corresponding one-way broadband transmission losses.

### 3.5. Pulse Compression Gains of Vocalizations from Baleen Whale Species

The mean pulse compression gains  $\gamma_{-6dB}$  and  $\gamma_{eq}$  of the vocalizations from the three baleen species, sei whale downsweep chirps, unidentified baleen whale species downsweep signals and fin whale 20-Hz pulses, are calculated (see Table 1). For comparison, the pulse compression gains of the 50-Hz bandwidth Tukey windowed [77] 1-s duration LFM signals centered at various frequencies from 300–2000 Hz commonly used in OAWRS (Ocean Acoustic Waveguide Remote Sensing) imaging [16,17,41,60,69,78] are also tabulated. For the Tukey windowed LFM signal, the equivalent pulse compression gain is equal to the time-bandwidth product. The  $\gamma_{-6dB}$  is smaller than the time-bandwidth product for the LFM signal and is a measure of the effective bandwidth due to bandwidth reduction from Tukey windowing. For the baleen species vocalizations, the  $\gamma_{-6dB}$  are larger than the corresponding equivalent pulse compression gains by roughly a factor of two and closer to the time-bandwidth products of these vocalization signals. The duration of each click in the minke whale pulse train is approximately 20 ms, which is roughly equivalent to the compressed pulse width of the sei whale downsweep chirps, so pulse compression analysis is not done here for minke whale click vocalizations.

**Table 1.** The potential pulse compression gains,  $\gamma_{-6dB}$  and  $\gamma_{eq}$ , of the baleen whale species vocalization signals with corresponding uncompressed pulse width  $\tau$ , spectral bandwidth  $B$  and time-bandwidth product  $\tau \cdot B$ . These parameters are also tabulated for a Tukey-window LFM pulse for comparison. The unidentified baleen whale species is indicated as UBWS.

	Fin	UBWS	Sei	Tukey-Windowed LFM
$\tau$ (s)	$1.0 \pm 0.3$	$1.9 \pm 0.4$	$2.2 \pm 0.4$	1.0
$B$ (Hz)	$11.2 \pm 0.5$	$30.1 \pm 7.2$	$54.5 \pm 7.6$	50.0
$\tau \cdot B$	$11.7 \pm 3.9$	$56.0 \pm 17.7$	$119.7 \pm 34.1$	50.0
$\tau_{c,-6dB}$ (ms)	$282 \pm 105$	$39 \pm 18$	$18 \pm 3$	24
$\tau_{c,eq}$ (ms)	$440 \pm 113$	$88 \pm 30$	$33 \pm 6$	20
$\gamma_{-6dB}$	$4.3 \pm 2.5$	$56 \pm 27$	$127 \pm 36$	41.2
$\gamma_{eq}$	$2.5 \pm 1.1$	$24 \pm 10$	$69 \pm 23$	50.6

Among the three baleen whale species investigated, the sei whale downsweep chirps have the largest pulse compression gain (Figure 8A–D), which is a factor of roughly 2.5-times larger than that of the unidentified baleen whale species downsweep calls and a factor of roughly 30-times larger than the fin 20-Hz pulses. This implies that the detection of sei whale chirp vocalizations can be significantly enhanced over ambient noise by employing pulse compression in passive marine mammal sensing systems. The pulse compression SNR enhancement is expected to be moderate for the unidentified baleen whale species downsweep vocalizations and insignificant for fin whale 20-Hz vocalizations.

The inter-pulse intervals of the fin whale, unidentified baleen whale species and sei whale vocalizations are roughly proportional to their pulse compression gains. The mean inter-pulse intervals of repetitive fin whale 20-Hz pulses, unidentified baleen whale species downsweep signals and sei whale downsweep chirp vocalizations are roughly 11, 29 and 52 s, respectively (Figure 9).

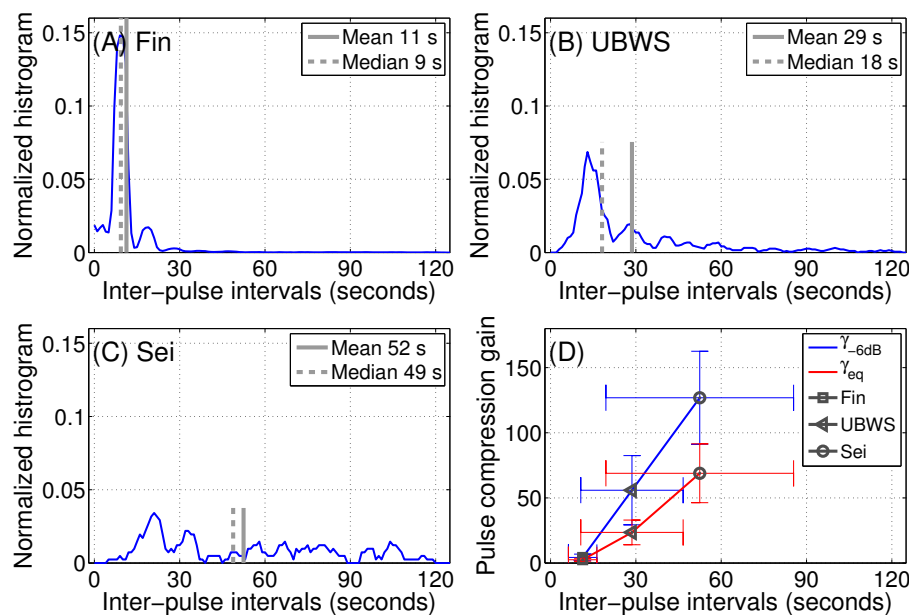


**Figure 9.** Distribution of Inter-Pulse Intervals (IPIs) for (A) fin whale 20-Hz pulses; (B) unidentified baleen whale species downsweep calls; and (C) sei whale downsweep chirps. For sei whales, the IPIs of their vocalizations in a doublet or triplet are not included. All IPIs larger than two minutes are excluded from the analysis; (D) The pulse compression gains,  $\gamma_{-6dB}$  and  $\gamma_{eq}$ , are plotted as a function of the IPIs. The IPI distributions are characterized by the following means and standard deviations, in units of seconds:  $11 \pm 5$  for fin whale,  $29 \pm 18$  for unidentified baleen whale species and  $52 \pm 33$  for sei whale.

#### 4. Discussion

The fin whale 20-Hz centered vocalization source level estimates obtained here in the Gulf of Maine compare well with previous estimates from other ocean areas, including the western Antarctic Peninsula [33], Northeast [34] and Central [79] Pacific Ocean. In general, the range of fin whale vocalization source level estimates from previous studies either overlap well with [5,80] or lie fully [33,34,79] within the range of fin whale vocalization source level estimates obtained here and shown in Figure 4E.

The mean value of the sei whale downsweep chirp vocalization source level distribution obtained here of  $173.5 \pm 3.2$  dB re 1  $\mu$ Pa at 1 m is smaller than previous estimates of sei whale downsweep vocalizations measured in the nearby continental shelf off New Jersey ( $179 \pm 4$  dB re 1  $\mu$ Pa at 1 m [35]).

The previously-reported [37] peak-to-peak source levels for Type c2 ( $181.6 \pm 6.6$  dB re 1  $\mu$ Pa at 1 m) and Type sd3 ( $176.7 \pm 4.2$  dB re 1  $\mu$ Pa at 1 m) averaged over minke whale click vocalizations have equivalent rms values of  $178.6 \pm 6.6$  dB re 1  $\mu$ Pa at 1 m and  $173.7 \pm 4.2$  dB re 1  $\mu$ Pa at 1 m, respectively, for comparison to the study here. These rms values from the previous study [37] for minke whales in the Gulf of Maine lie well within the span of minke whale click vocalization rms source levels found here, which range from roughly 160–190 dB re 1  $\mu$ Pa at 1 m.

Our stochastic broadband transmission loss model calculations have been extensively calibrated and verified with thousands of one-way and two-way transmission loss measurements made during the same Gulf of Maine 2006 experiment at the same time and location [16,17,41]. It is also verified by roughly one hundred two-way transmission loss measurements made from calibrated targets with known scattering properties [59] during the same experiment at the same time and location, indicating that our transmission loss measurements did not create a bias. Therefore, the observed difference between this study and previous ones is not likely caused by biased transmission loss measurements.

The POAWRS coherent hydrophone array's instantaneous marine mammal detection region extends over 100,000 km<sup>2</sup>, which is a factor of roughly 100-times larger than that of a single

omnidirectional hydrophone. The vocalizing marine mammal population from each species instantaneously detected by POAWRS is expected to be larger than that of a single omnidirectional hydrophone. Based on historical visual surveys [81,82], the fall season areal population density of marine mammals in units of abundance per 1000 km<sup>2</sup> in their densest areas on or near northern Georges Bank (see Figures 1 and 2 of [1] for the locations of these dense areas during the experiment) is expected to range from roughly 10–22 for fin whales, 4–16 for minke whales and 3–24 for sei whales (refer to Supplementary Information Section IV of [1] for details). The vocalization source level estimates obtained here represent an average over multiple vocalizing marine mammal individuals for each species within the roughly 100,000-km<sup>2</sup> POAWRS detection region.

Baleen whale vocalizations are generally regarded as communication or contact signals for purposes such as coordinated feeding, migration and mating. Baleen whales are not known to produce sounds for echolocation or navigation, which is a capability in toothed whales. Some studies have suggested a potential for echolocation [25,83] or navigation [25,84] in some select baleen whale species, but is highly dependent on vocalization type [83], environmental and prey conditions [25], and they do not consider pulse compression gains since this ability is not known to be present in baleen whales. Here, the pulse compression gains are quantified for passive acoustic marine mammal sensing systems that use pulse compressions to enhance whale vocalization signal detection or bearing-time estimation for whale localization.

## 5. Conclusions

The vocalization source level distributions and pulse compression gains have been estimated for fin whale, sei whale, minke whale and an unidentified baleen whale species in the Gulf of Maine. The vocalization source level distributions are based on measurements made using a large-aperture densely-sampled coherent hydrophone array system that provides high SNR in signal detection, large sample sizes, as well as robust array-based methods for whale localization using vocalization bearing-time measurements over areas spanning 100,000 km<sup>2</sup>. An azimuth and range-dependent ocean acoustic propagation model calibrated for the Gulf of Maine environment was employed to correct the received vocalization pressure levels from various whale species with transmission losses. The whale species vocalization source level distributions are found to be characterized by the following rms means and standard deviations, in units of dB re 1 µPa at 1 m: 181.9 ± 5.2 for fin whale 20-Hz pulses, 173.5 ± 3.2 for sei whale downsweep chirps, 177.7 ± 5.4 for minke whale pulse trains and 169.6 ± 3.5 for an unidentified baleen whale species downsweep calls. The baleen whale species vocalization equivalent pulse compression gains have been estimated and found to be roughly 2.5 ± 1.1 for fin whale 20-Hz pulses, 24 ± 10 for the unidentified baleen whale species downsweep signals and 69 ± 23 for sei whale downsweep chirps. The pulse compression gains, source levels and inter-pulse intervals estimated here can be used as inputs for modeling the signal-to-noise ratios and hence detection regions of vocalizations from baleen whale species received passively on underwater acoustic sensing systems [1,2], as well as for assessing the communication ranges of baleen whales.

**Acknowledgments:** Permission for this National Oceanographic Partnership Program experiment was given in the Office of Naval Research document 5090 Ser 321RF/096/06. This research was supported by the U.S. Office of Naval Research (Ocean Acoustics Program), the U.S. National Science Foundation, the National Oceanographic Partnership Program, the U.S. Presidential Early Career Award for Scientists and Engineers, the Alfred P. Sloan Foundation, the Census of Marine Life and Northeastern University.

**Author Contributions:** Data analysis and interpretation conducted primarily by Delin Wang, with contributions from Wei Huang, Heriberto Garcia and Purnima Ratilal. Delin Wang wrote the paper with contributions from Purnima Ratilal.

**Conflicts of Interest:** The authors declare no conflict of interest. The founding sponsors had no role in the design of the study; in the collection, analyses or interpretation of data; in the writing of the manuscript; nor in the decision to publish the results.

## Abbreviations

The following abbreviations are used in this manuscript:

SNR	Signal-to-Noise Ratio
POAWRS	Passive Ocean Acoustic Waveguide Remote Sensing
OAWRS	Ocean Acoustic Waveguide Remote Sensing
RAM	Range-dependent Acoustic propagation Model
GPS	Global Positioning System
XBT	Expendable Bathythermograph
CTD	Conductivity-Temperature-Depth
PCA	Principle Component Analysis
MAT	Moving Array Triangulation
MMSE	Minimum Mean Square Error
rms	root mean squared
PCG	Pulse Compression Gain
LFM	Linear Frequency Modulated
EDT	Eastern Daylight Time
IPI	Inter-Pulse Interval
UBWS	Unidentified Baleen Whale Species

## References

- Wang, D.; Garcia, H.; Huang, W.; Tran, D.D.; Jain, A.D.; Yi, D.H.; Gong, Z.; Jech, J.M.; Godø, O.R.; Makris, N.C.; Ratilal, P. Vast assembly of vocal marine mammals from diverse species on fish spawning ground. *Nature* **2016**, *531*, 366–370.
- Gong, Z.; Jain, A.D.; Tran, D.D.; Yi, D.H.; Wu, F.; Zorn, A.; Ratilal, P.; Makris, N.C. Ecosystem scale acoustic sensing reveals humpback whale behavior synchronous with herring spawning processes and re-evaluation finds no effect of sonar on humpback song occurrence in the Gulf of Maine in Fall 2006. *PLoS ONE* **2014**, *9*, e104733.
- Tran, D.D.; Huang, W.; Bohn, A.C.; Wang, D.; Gong, Z.; Makris, N.C.; Ratilal, P. Using a coherent hydrophone array for observing sperm whale range, classification, and shallow-water dive profiles. *J. Acoust. Soc. Am.* **2014**, *135*, 3352–3363.
- Kay, S.M. *Fundamentals of Statistical Signal Processing, Vol. II: Detection Theory*; Prentice Hall: Upper Saddle River, NJ, USA, 1998.
- Watkins, W.A.; Tyack, P.; Moore, K.E.; Bird, J.E. The 20-Hz signals of finback whales (*Balaenoptera physalus*). *J. Acoust. Soc. Am.* **1987**, *82*, 1901–1912.
- Edds, P.L. Characteristics of finback *Balaenoptera physalus* vocalizations in the St. Lawrence Estuary. *Bioacoustics* **1988**, *1*, 131–149.
- Nieukirk, S.L.; Mellinger, D.K.; Moore, S.E.; Klinck, K.; Dziak, R.P.; Goslin, J. Sounds from airguns and fin whales recorded in the mid-Atlantic Ocean, 1999–2009. *J. Acoust. Soc. Am.* **2012**, *131*, 1102–1112.
- Thompson, P.O.; Findley, L.T.; Vidal, O. 20-Hz pulses and other vocalizations of fin whales, *Balaenoptera physalus*, in the Gulf of California, Mexico. *J. Acoust. Soc. Am.* **1992**, *92*, 3051–3057.
- Rankin, S.; Barlow, J. Vocalizations of the sei whale *Balaenoptera borealis* off the Hawaiian Islands. *Bioacoustics* **2007**, *16*, 137–145.
- Baumgartner, M.F.; Van Parijs, S.M.; Wenzel, F.W.; Tremblay, C.J.; Esch, H.C.; Warde, A.M. Low frequency vocalizations attributed to sei whales (*Balaenoptera borealis*). *J. Acoust. Soc. Am.* **2008**, *124*, 1339–1349.
- Baumgartner, M.F.; Fratantoni, D.M. Diel periodicity in both sei whale vocalization rates and the vertical migration of their copepod prey observed from ocean gliders. *Limnol. Oceanogr.* **2008**, *53*, 2197–2209.
- Edds-Walton, P.L. Vocalizations of menke whales *Balaenoptera acutorostrata* in the St. Lawrence Estuary. *Bioacoustics* **2000**, *11*, 31–50.
- Mellinger, D.K.; Carson, C.D.; Clark, C.W. Characteristics of minke whale (*Balaenoptera acutorostrata*) pulse trains recorded near Puerto Rico. *Mar. Mamm. Sci.* **2000**, *16*, 739–756.

14. Risch, D.; Clark, C.W.; Dugan, P.J.; Popescu, M.; Siebert, U.; Van Parijs, S.M. Minke whale acoustic behavior and multi-year seasonal and diel vocalization patterns in Massachusetts Bay, USA. *Mar. Ecol. Prog. Ser.* **2013**, *489*, 279–295.
15. Berchok, C.L.; Bradley, D.L.; Gabrielson, T.B. St. Lawrence blue whale vocalizations revisited: Characterization of calls detected from 1998 to 2001. *J. Acoust. Soc. Am.* **2006**, *120*, 2340–2354.
16. Gong, Z.; Andrews, M.; Jagannathan, S.; Patel, R.; Jech, J.M.; Makris, N.C.; Ratilal, P. Low-frequency target strength and abundance of shoaling Atlantic herring (*Clupea harengus*) in the Gulf of Maine during the Ocean Acoustic Waveguide Remote Sensing 2006 Experiment. *J. Acoust. Soc. Am.* **2010**, *127*, 104–123.
17. Makris, N.C.; Ratilal, P.; Jagannathan, S.; Gong, Z.; Andrews, M.; Bertsatos, I.; Godø, O.R.; Nero, R.W.; Jech, J.M. Critical population density triggers rapid formation of vast oceanic fish shoals. *Science* **2009**, *323*, 1734–1737.
18. Andrews, M.; Chen, T.; Ratilal, P. Empirical dependence of acoustic transmission scintillation statistics on bandwidth, frequency, and range in New Jersey continental shelf. *J. Acoust. Soc. Am.* **2009**, *125*, 111–124.
19. Urick, R.J. *Principles of Underwater Sound*; McGraw-Hill: New York, NY, USA, 1983; pp. 29–65, 343–366.
20. Burdic, W.S. *Underwater Acoustic System Analysis*; Prentice Hall: Upper Saddle River, NJ, USA, 1984; pp. 322–360.
21. Jensen, F.B.; Kuperman, W.A.; Porter, M.B.; Schmidt, H. *Computational Ocean Acoustics*; Springer: Berlin, Germany, 2011; pp. 708–713.
22. Gong, Z.; Tran, D.D.; Ratilal, P. Comparing passive source localization and tracking approaches with a towed horizontal receiver array in an ocean waveguide. *J. Acoust. Soc. Am.* **2013**, *134*, 3705–3720.
23. Gong, Z.; Ratilal, P.; Makris, N.C. Simultaneous localization of multiple broadband non-impulsive acoustic sources in an ocean waveguide using the array invariant. *J. Acoust. Soc. Am.* **2015**, *138*, 2649–2667.
24. Lee, S.; Makris, N.C. The array invariant. *J. Acoust. Soc. Am.* **2006**, *119*, 336–351.
25. Yi, D.H.; Makris, N.C. Feasibility of Acoustic Remote Sensing of Large Herring Shoals and Seafloor by Baleen Whales. *Remote Sens.* **2016**, *8*, doi:10.3390/rs8090693.
26. Buckland, S.T.; Anderson, D.R.; Burnham, K.P.; Laake, J.L.; Borchers, D.L.; Thomas, L. *Introduction to Distance Sampling Estimating Abundance of Biological Populations*; Oxford University Press: Oxford, UK, 2001.
27. Küsel, E.T.; Mellinger, D.K.; Thomas, L.; Marques, T.A.; Moretti, D.; Ward, J. Cetacean population density estimation from single fixed sensors using passive acoustics. *J. Acoust. Soc. Am.* **2011**, *129*, 3610–3622.
28. Martin, S.W.; Marques, T.A.; Thomas, L.; Morrissey, R.P.; Jarvis, S.; DiMarzio, N.; Moretti, D.; Mellinger, D.K. Estimating minke whale (*Balaenoptera acutorostrata*) boing sound density using passive acoustic sensors. *Mar. Mammal Sci.* **2013**, *29*, 142–158.
29. Marques, T.A.; Munger, L.; Thomas, L.; Wiggins, S.; Hildebrand, J.A. Estimating North Pacific right whale *Eubalaena japonica* density using passive acoustic cue counting. *Endanger. Species Res.* **2011**, *13*, 163–172.
30. Marques, T.A.; Thomas, L.; Martin, S.W.; Mellinger, D.K.; Ward, J.A.; Moretti, D.J.; Harris, D.; Tyack, P.L. Estimating animal population density using passive acoustics. *Biol. Rev.* **2013**, *88*, 287–309.
31. Croll, D.A.; Clark, C.W.; Calambokidis, J.; Ellison, W.T.; Tershy, B.R. Effect of anthropogenic low-frequency noise on the foraging ecology of Balaenoptera whales. *Anim. Conserv.* **2001**, *4*, 13–27.
32. Nowacek, D.P.; Thorne, L.H.; Johnston, D.W.; Tyack, P.L. Responses of cetaceans to anthropogenic noise. *Mammal Rev.* **2007**, *37*, 81–115.
33. Širović, A.; Hildebrand, J.A.; Wiggins, S.M. Blue and fin whale call source levels and propagation range in the Southern Ocean. *J. Acoust. Soc. Am.* **2007**, *122*, 1208–1215.
34. Weirathmueller, M.J.; Wilcock, W.S.D.; Soule, D.C. Source levels of fin whale 20 Hz pulses measured in the Northeast Pacific Ocean. *J. Acoust. Soc. Am.* **2013**, *133*, 741–749.
35. Newhall, A.E.; Lin, Y.T.; Lynch, J.F.; Baumgartner, M.F.; Gawarkiewicz, G.G. Long distance passive localization of vocalizing sei whales using an acoustic normal mode approach. *J. Acoust. Soc. Am.* **2012**, *131*, 1814–1825.
36. Gedamke, J.; Costa, D.P.; Dunstan, A. Localization and visual verification of a complex minke whale vocalization. *J. Acoust. Soc. Am.* **2001**, *109*, 3038–3047.
37. Risch, D.; Siebert, U.; Van Parijs, S.M. Individual calling behaviour and movements of North Atlantic minke whales (*Balaenoptera acutorostrata*). *Behaviour* **2014**, *151*, 1335–1360.
38. Cummings, W.C.; Thompson, P.O. Underwater sounds from the blue whale, *Balaenoptera musculus*. *J. Acoust. Soc. Am.* **1971**, *50*, 1193–1198.



39. Wiggins, S.M.; Oleson, E.M.; McDonald, M.A.; Hildebrand, J.A. Blue whale (*Balaenoptera musculus*) diel call patterns offshore of Southern California. *Aquat. Mamm.* **2005**, *31*, 161–168.
40. Oleson, E.M.; Calambokidis, J.; Burgess, W.C.; McDonald, M.A.; LeDuc, C.A.; Hildebrand, J.A. Behavioral context of call production by eastern North Pacific blue whales. *MEPS* **2007**, *330*, 269–284.
41. Tran, D.D.; Andrews, M.; Ratilal, P. Probability distribution for energy of saturated broadband ocean acoustic transmission: Results from Gulf of Maine 2006 experiment. *J. Acoust. Soc. Am.* **2012**, *132*, 3659–3672.
42. Collins, M.D. A split-step Padé solution for the parabolic equation method. *J. Acoust. Soc. Am.* **1993**, *93*, 1736–1742.
43. Skolnik, M.I. *Introduction to Radar Systems*; Electrical Engineering Series; McGraw Hill: New York, NY, USA, 2001.
44. Kroszczynski, J.J. Pulse compression by means of linear-period modulation. *Proc. IEEE* **1969**, *57*, 1260–1266.
45. Stafford, K.M.; Fox, C.G.; Clark, D.S. Long-range acoustic detection and localization of blue whale calls in the northeast Pacific Ocean. *J. Acoust. Soc. Am.* **1998**, *104*, 3616–3625.
46. Mellinger, D.K.; Clark, C.W. Recognizing transient low-frequency whale sounds by spectrogram correlation. *J. Acoust. Soc. Am.* **2000**, *107*, 3518–3529.
47. Mellinger, D.K.; Clark, C.W. Methods for automatic detection of mysticete sounds. *Mar. Freshw. Behav. Physiol.* **1997**, *29*, 163–181.
48. Flore, S.; Adam, O.; Motsch, J.F.; Guinet, C. Definition of the Antarctic and pygmy blue whale call templates. Application to fast automatic detection. *Can. Acoust.* **2008**, *36*, 93–103.
49. Haedrich, R.L. Bigelow and Schroeder's Fishes of the Gulf of Maine. *Copeia* **2003**, *2003*, 422–423.
50. Jain, A.D.; Ignisca, A.; Yi, D.H.; Ratilal, P.; Makris, N.C. Feasibility of ocean acoustic waveguide remote sensing (OAWRS) of Atlantic cod with seafloor scattering limitations. *Remote Sens.* **2013**, *6*, 180–208.
51. Nelson, G.A.; Ross, M.R. Biology and population changes of northern sand lance (*Ammodytes dubius*) from the Gulf of Maine to the Middle Atlantic Bight. *J. Northwest Atl. Fish. Sci.* **1991**, *11*, 11–27.
52. Overholtz, W.J.; Link, J.S. Consumption impacts by marine mammals, fish, and seabirds on the Gulf of Maine–Georges Bank Atlantic herring (*Clupea harengus*) complex during the years 1977–2002. *ICES J. Mar. Sci.* **2007**, *64*, 83–96.
53. Overholtz, W.J.; Jacobson, L.D.; Melvin, G.D.; Cieri, M.; Power, M.; Libby, D.; Clark, K. Stock assessment of the Gulf of Maine–Georges Bank Atlantic herring complex, 2003. *Northeast Fish. Sci. Cent. Ref. Doc.* **2004**, *4*, 1–290.
54. Melvin, G.D.; Stephenson, R.L. The dynamics of a recovering fish stock: Georges Bank herring. *ICES J. Mar. Sci.* **2007**, *64*, 69–82.
55. Read, A.J.; Brownstein, C.R. Considering other consumers: Fisheries, predators, and Atlantic herring in the Gulf of Maine. *Conserv. Ecol.* **2003**, *7*, 2.
56. Jech, J.M.; Stroman, F. Aggregative patterns of pre-spawning Atlantic herring on Georges Bank from 1999–2010. *Aquat. Living Resour.* **2012**, *25*, 1–14.
57. Klaer, N. CIE Reviewer's Independent Report. In Proceedings of the 54th Northeast Regional Stock Assessment Workshop, Woods Hole, MA, USA, 5–9 June 2012.
58. Overholtz, W. The Gulf of Maine–Georges Bank Atlantic herring (*Clupea harengus*): Spatial pattern analysis of the collapse and recovery of a large marine fish complex. *Fish. Res.* **2002**, *57*, 237–254.
59. Jagannathan, S.; Küsel, E.T.; Ratilal, P.; Makris, N.C. Scattering from extended targets in range-dependent fluctuating ocean-waveguides with clutter from theory and experiments. *J. Acoust. Soc. Am.* **2012**, *132*, 680–693.
60. Jagannathan, S.; Bertsatos, I.; Symonds, D.; Chen, T.; Nia, H.T.; Jain, A.D.; Andrews, M.; Gong, Z.; Nero, R.; Ngor, L.; et al. Ocean acoustic waveguide remote sensing (OAWRS) of marine ecosystems. *Mar. Ecol. Progr. Ser.* **2009**, *395*, 137–160.
61. Center, N.F.S. Atlantic herring stock assessment for 2012. In Proceedings of the 54th Northeast Regional Stock Assessment Workshop (54th SAW), Woods Hole, MA, USA, 5–9 June 2012.
62. Jech, J.M.; Price, V.; Chavez-Rosales, S.; Michaels, W. Atlantic herring (*Clupea harengus*) demographics in the Gulf of Maine from 1998 to 2012. *J. Northwest Atl. Fish. Sci.* **2015**, *47*, 57–74.
63. Becker, K.; Preston, J. The ONR five octave research array (FORA) at Penn State. *Proc. IEEE* **2003**, *5*, 2607–2610.

64. Andrews, M.; Gong, Z.; Ratilal, P. High resolution population density imaging of random scatterers with the matched filtered scattered field variance. *J. Acoust. Soc. Am.* **2009**, *126*, 1057–1068.
65. Shapiro, A.D.; Wang, C. A versatile pitch tracking algorithm: From human speech to killer whale vocalizations. *J. Acoust. Soc. Am.* **2009**, *126*, 451–459.
66. Wang, C.; Seneff, S. Robust pitch tracking for prosodic modeling in telephone speech. In Proceedings of the 2000 IEEE International Conference on Acoustics, Speech, and Signal Processing, Piscataway, NJ, USA, 5–9 June 2000; Volume 3, pp. 1343–1346.
67. Jolliffe, I. *Principal Component Analysis*, 2nd ed.; Wiley Online Library: New York, NY, USA, 2002; pp. 11–31.
68. Kanungo, T.; Mount, D.M.; Netanyahu, N.S.; Piatko, C.D.; Silverman, R.; Wu, A.Y. An efficient k-means clustering algorithm: Analysis and implementation. *IEEE Trans. Pattern Anal. Mach. Intell.* **2002**, *24*, 881–892.
69. Ratilal, P.; Lai, Y.; Symonds, D.T.; Ruhlmann, L.A.; Preston, J.R.; Scheer, E.K.; Garr, M.T.; Holland, C.W.; Goff, J.A.; Makris, N.C. Long range acoustic imaging of the continental shelf environment: The Acoustic Clutter Reconnaissance Experiment 2001. *J. Acoust. Soc. Am.* **2005**, *117*, 1977–1998.
70. Andrews, M.; Gong, Z.; Ratilal, P. Effects of multiple scattering, attenuation and dispersion in waveguide sensing of fish. *J. Acoust. Soc. Am.* **2011**, *130*, 1253–1271.
71. Kinsler, L.E.; Frey, A.R.; Coppens, A.B.; Sanders, J.V. *Fundamentals of Acoustics*, 4th ed.; Wiley-VCH: New York, NY, USA, 1999.
72. Madsen, P.T.; Wahlberg, M. Recording and quantification of ultrasonic echolocation clicks from free-ranging toothed whales. *Deep Sea Res. Part I* **2007**, *54*, 1421–1444.
73. Goodman, J.W. *Statistical Optics*; John Wiley & Sons: Hoboken, NJ, USA, 2015.
74. Makris, N.C. The effect of saturated transmission scintillation on ocean acoustic intensity measurements. *J. Acoust. Soc. Am.* **1996**, *100*, 769–783.
75. McDonald, M.A.; Hildebrand, J.A.; Webb, S.C. Blue and fin whales observed on a seafloor array in the Northeast Pacific. *J. Acoust. Soc. Am.* **1995**, *98*, 712–721.
76. Croll, D.A.; Clark, C.W.; Acevedo, A.; Tershy, B.; Flores, S.; Gedamke, J.; Urban, J. Bioacoustics: Only male fin whales sing loud songs. *Nature* **2002**, *417*, doi:10.1038/417809a.
77. Oppenheim, A.V.; Schaffer, R.W. *Discrete-Time Signal Processing*; Pearson Higher Education: New York, NY, USA, 2010.
78. Galinde, A.; Donabed, N.; Andrews, M.; Lee, S.; Makris, N.C.; Ratilal, P. Range-dependent waveguide scattering model calibrated for bottom reverberation in a continental shelf environment. *J. Acoust. Soc. Am.* **2008**, *123*, 1270–1281.
79. Northrop, J.; Cummings, W.C.; Thompson, P.O. 20-Hz Signals Observed in the Central Pacific. *J. Acoust. Soc. Am.* **1968**, *43*, 383–384.
80. Charif, R.A.; Mellinger, D.K.; Dunsmore, K.J.; Fristrup, K.M.; Clark, C.W. Estimated source levels of fin whale (*Balaenoptera physalus*) vocalizations: Adjustments for surface interference. *Mar. Mamm. Sci.* **2002**, *18*, 81–98.
81. Battista, T.; Clark, R.; Pittman, S. *An Ecological Characterization of the Stellwagen Bank National Marine Sanctuary Region: Oceanographic, Biogeographic, and Contaminants Assessment*; Center for Coastal Monitoring and Assessment (CCMA), NOAA/NOS/NCCOS: Silver Spring, MD, USA, 2006.
82. Payne, P.M.; Selzer, L.A.; Knowlton, A.R. *Distribution and Density of Cetaceans, Marine Turtles, And Seabirds in the Shelf Waters of the Northeastern United States, June 1980-December 1983, Based on Shipboard Observations*; Manomet Bird Observatory: Cumberland, ME, USA, 1984.
83. Stimpert, A.K.; Wiley, D.N.; Au, W.W.; Johnson, M.P.; Arsenault, R. ‘Megapclicks’: Acoustic click trains and buzzes produced during night-time foraging of humpback whales (*Megaptera novaeangliae*). *Biol. Lett.* **2007**, *3*, 467–470.
84. Ellison, W.T.; Clark, C.W.; Bishop, G.C. Potential use of surface reverberation by bowhead whales, *Balaena mysticetus*, in under-ice navigation: Preliminary considerations. *Rep. Int. Whal. Comm.* **1987**, *37*, 329–332.

